THE JOURNAL OF PHYSICAL CHEMISTRY B

Article

Cite This: J. Phys. Chem. B 2018, 122, 3441−3446

pubs.acs.org/JPCB

Critical Point Confluence Phenomenon

Frank H. Stillinger*

Department of Chemistry, Princeton University, Princeton, New Jersey 08544, United States

ABSTRACT: Experimental observation of coexisting isotropic chiral liquids for a single molecular substance has motivated creation of a simple lattice model to investigate phase transitions in such systems. Specifically, this model permits the simultaneous existence of two distinct types of critical points, the familiar liquid−vapor case, and a case involving spontaneous chiral symmetry breaking within the fluid system. The molecular interactions involved may extend beyond nearest neighbor lattice cells. The mean field approximation has been invoked to attain explicit results, which include a description of the singular situation for which the two critical points undergo confluence in the temperature−density plane. In particular, this confluence enhances the chiral symmetry breaking phenomenon, leading to a modified critical exponent.

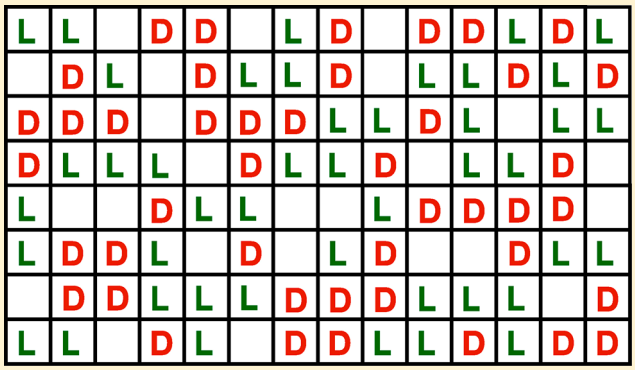

I. INTRODUCTION

Critical phenomena exhibited by thermally equilibrated many-body systems have continued to generate widespread interest in both the experimental and the theoretical communities. One of the more unusual circumstances among the liquid-state observations involves the appearance of a pair of critical points (solution consolute points) at upper and lower temperature limits of isobaric closed-loop coexistence curves.[1,2] The size and shape of these equilibrium coexistence curves, and therefore the proximity of the critical points, can be manipulated by varying the applied pressure and the overall chemical composition of the system. In principle, such conditions might exist that could bring the pair of critical points arbitrarily close, and thus to converge to a "double critical point".

Recent experimental observations have led to the possibility of an analogous, but qualitatively distinct, pair of fluid-state critical points exhibited by single component molecular systems in thermal equilibrium. Specifically, examples have been identified of coexisting isotropic chiral liquids that become visibly distinguishable under polarized light, with clearly identifiable contact interfaces.[3,4] Although not yet directly observed, it is reasonable to assume that a set of flexible molecular substances could be identified that under proper equilibrium conditions would present both a conventional liquid−vapor critical point, as well as a chiral-symmetry-breaking critical point.

A three-dimensional continuum flexible tetramer model has recently been introduced and analyzed by molecular dynamics simulation, specifically to illustrate the phenomenon of spontaneous chiral symmetry breaking.[5] The intramolecular interactions assigned to each tetramer create a pair of mirror-image stable structures for the isolated molecules, between which relatively high energy transition states permit chiral inversions to occur, given sufficient excitation energy. The model also includes a simplified intermolecular pair interaction with parameter control that allows spanning both enantiopure (equal chirality) and racemic (opposite chirality) preferences. With the former choice, lowering the temperature isochorically in the simulations produced a continuous phase transition critical point from a single racemic fluid phase to coexistence of immiscible isotropic chiral fluids. The presence in the model also of overall short-range attraction between tetramers regardless of their chirality certainly leads as well to the possibility of a conventional racemic-liquid, racemic-vapor critical point, at an appropriate temperature-density state.

To produce a stripped-down statistical model exhibiting a pair of critical points analogous to those expected for the detailed tetramer model, a conceptually simple lattice version has been created. Its description appears in the following section II. Section III introduces a mean field approximation to produce at least a qualitatively valid view of the chiral-symmetry-breaking phase change exhibited by that lattice model, which is then detailed in section IV. Section V applies that mean field approximation to description of the liquid−vapor phase transition and its own critical point. The nature of the possible confluence of these two critical points forms the subject of section VI, leading up to the final section VII that contains concluding remarks.

II. LATTICE MODEL

The present investigation will focus on a three-dimensional Bravais lattice arrangement of M equivalent cells, subject to

Special Issue: Benjamin Widom Festschrift

Received: October 23, 2017
Revised: November 28, 2017
Published: November 28, 2017

DOI: 10.1021/acs.jpcb.7b10498
J. Phys. Chem. B 2018, 122, 3441−3446

periodic boundary conditions. Each cell may be empty or, alternatively, may contain at most a single particle. Because this lattice model is intended as a coarse-grained version of the chiral tetramer model,[5] the instantaneous status of each cell i ($1 \le i \le M$) will be identified by a discrete occupancy variable ν_i, whose three distinct values are assigned as follows:

$$\begin{aligned} \nu_i &= -1 \text{ (left-handed chiral occupant)}, \\ &= 0 \text{ (empty cell)}, \\ &= +1 \text{ (right-handed chiral occupant)} \end{aligned} \tag{1}$$

The overall numbers of left-handed (N_-) and of right-handed (N_+) enantiomers therefore are

$$\begin{aligned} N_- &= \sum_{i=1}^{M} \nu_i(\nu_i - 1)/2 \\ N_+ &= \sum_{i=1}^{M} \nu_i(\nu_i + 1)/2 \end{aligned} \tag{2}$$

so that the overall particle count on the lattice is

$$N = N_+ + N_- = \sum_{i=1}^{M} \nu_i^2 \tag{3}$$

The drastic configurational simplification produced by transforming to the lattice model eliminates the possibility of realistically describing crystallization transitions that arise in the foregoing more detailed tetramer model.[5]

A potential energy function $\Phi(\nu_1,\nu_2,...,\nu_M)$ is assigned to each cell occupancy pattern. This must be invariant to overall mirror inversion symmetry, thus requiring

$$\Phi(\nu_1,\nu_2,...,\nu_M) = \Phi(-\nu_1,-\nu_2,...,-\nu_M) \tag{4}$$

The pairwise-additive intermolecular potentials contained in the prior tetramer model[5] are a feature to be transcribed qualitatively into the present coarse-grained lattice description. That requirement can be implemented by accepting the following Φ format:

$$\Phi(\nu_1,\nu_2,...,\nu_M) = \sum_{i=2}^{M} \sum_{j=1}^{i-1} [\nu_i^2\nu_j^2\varphi_J(r_{ij}) + \nu_i\nu_j\varphi_K(r_{ij})] \tag{5}$$

where r_{ij} stands for the scalar distance between the centers of cells i and j. Here the role of particle pair interaction function φ_J is to be primarily negative, so as to provide an overall attraction between the particles, regardless of their chirality. By contrast, φ_K is present to distinguish between the chiralities of the two particles involved; if this function is primarily positive it favors opposite chiralities (racemic preference), but if it is primarily negative, it favors equal chiralities (enantiopure preference). To conform to the foregoing tetramer model, it will be assumed that the spatial variations of φ_J and φ_K are no longer-ranged than r_{ij}^{-6}.

The three distinct values of the cell occupancy variables ν_i can be interpreted as defining a spin-1 Ising model. Consequently, this description places the present model in close relation to the "tricritical Ising model" that was introduced to explain the low temperature phase behavior of He^3–He^4 mixtures.[6] However, that earlier spin-1 Ising model only involved nearest-neighbor interactions, in contrast to the possibly longer range contributions contained in eq 5. It is also important to note that the intrinsic chirality inversion described by spin sign change, eqs 1 and 4, does not have a correspondingly precise binary symmetry for the helium isotope mixtures. This inequivalence indicates that critical point confluence in the present lattice model does not necessarily imply the appearance of the same type of confluence for observable phase behavior of helium mixtures.

A principle objective is evaluation of a canonical partition function for a fixed M, and a fixed total number of particles $N \le M$. Each particle present can spontaneously undergo chiral inversion, so N_+ (and thus N_-) can vary between obvious extreme limits. The relevant configurational part of the classical canonical partition function at absolute temperature T can be expressed as follows:

$$\begin{aligned} Z(M,N,T) &= \omega^N \sum_{\{\nu_i\}}^{(M,N)} \exp[-\Phi(\nu_1,...,\nu_M)/k_BT] \\ &\equiv \exp[-F(M,N,T)/k_BT] \end{aligned} \tag{6}$$

where F is the corresponding configurational Helmholtz free energy, ω is the cell volume, and k_B is Boltzmann's constant. The summation covers all occupancy configurations subject to the fixed-M and fixed-N constraints.

III. MEAN FIELD DESCRIPTION

As already indicated, the lattice model description presented in the preceding section II amounts to a special case of a three-dimensional spin-1 Ising model. To extract useful information straightforwardly from its configurational partition function eq 6, it is necessary to impose a basic simplifying approximation. For present purposes the mean field approach suffices. This presumes that each particle interacts via φ_J and φ_K with its local environment that is assumed to be compositionally equivalent to the system-wide macroscopic densities of left-handed and right-handed particles. That approximation implicitly supposes that the overall system at fixed M and N is occupied by a single homogeneous phase, a presumption that needs to be revisited later. Such a mean field assumption causes the canonical configurational partition function eq 6 to undergo a drastic simplification to the following form in the large-system limit:

$$\begin{aligned} Z(M,N,T) \approx \omega^N \sum_{N_+=0}^{N} &\frac{M!}{(M-N)!N_+!N_-!} \\ &\times \exp\{-[JN^2 + K(N_+ - N_-)^2]/2Mk_BT\} \end{aligned} \tag{7}$$

Here the mean-field coupling parameters J and K are determined by the relations

$$\begin{aligned} J &= \sum_{j=2}^{M} \phi_J(r_{1j}) \\ K &= \sum_{j=2}^{M} \phi_K(r_{1j}) \end{aligned} \tag{8}$$

In a situation where $J < 0$ and $K = 0$ the system would exhibit a single critical point, involving liquid–vapor separation. The contrasting situation where $J = 0$ and $K < 0$ would also generate a single critical point, but instead involving separation of opposite chirality phases of equal number densities. Of course,

DOI: 10.1021/acs.jpcb.7b10498
J. Phys. Chem. B 2018, 122, 3441–3446

the objective of the present analysis is to describe the simultaneous presence of both critical point types.

For the purpose of algebraic clarity, let intensive variable $-1 \leq x \leq +1$ measure a configuration's deviation from racemic symmetry:

$$N_+ = (1 + x)N/2$$
$$N_- = (1 - x)N/2 \tag{9}$$

The configurational free energy emerging from eq 7, in the large-system limit of interest, is dominated by the maximum term (or terms) of the summand. Using Stirling's formula for factorials, this immediately produces the following expression for the negative of the configurational free energy per particle:

$$\begin{aligned} -F(M,N,T)/Nk_BT &\approx \ln \omega + \left(\frac{M}{N}\right)\ln\left(\frac{M}{N}\right) - \left(\frac{M}{N} - 1\right)\ln\left(\frac{M}{N} - 1\right) \\ &+ \ln 2 - \left(\frac{JN}{2Mk_BT}\right) + \frac{1}{2}\underbrace{\max}_{x}\left\{-(1 + x)\ln(1 + x)\right. \\ &\left. - (1 - x)\ln(1 - x) - \left(\frac{KN}{Mk_BT}\right)x^2\right\} \end{aligned} \tag{10}$$

The maxima with respect to x (i.e., free energy minima) can be located by setting the x derivative of this last expression equal to zero (while verifying that the corresponding second derivative is negative). This leads to the following determining formula satisfied by the extremal x values:

$$\frac{1 + x}{1 - x} = \exp\left[-\left(\frac{2K\rho}{k_BT}\right)x\right] \tag{11}$$

where $\rho = N/M$ is the particle number density on a per-cell basis.

It should be mentioned once again that the applicability of eqs 10 and 11 rely on the assumption that the system consists of a single homogeneous phase. As will be detailed below, this will be the case if the occupation density ρ is sufficiently large.

IV. CHIRAL SYMMETRY BREAKING TRANSITION

When $K \geq 0$, the only (real) solution to eq 11 is $x = 0$, the expected racemic state at all temperatures. Changing the sign of K, however, leads to the appearance of chiral symmetry breaking within the homogeneous racemic fluid, provided that $|K|$ is substantially larger than $|J|$, and that the temperature is sufficiently low. Figure 1 presents the corresponding numerical results from eq 11 for x versus the dimensionless parameter $K\rho/k_BT$. As this parameter declines below -1, the free energy minimum at $x = 0$ continuously transforms into a maximum that immediately becomes surrounded by a symmetric pair of free energy minima. These latter are the indicators of the spontaneous chiral symmetry breaking transition whose critical point temperature $T_\pm$ in the mean field approximation therefore occurs at

$$k_BT_\pm = -K\rho \tag{12}$$

where particle coverage density $\rho = N/M$ refers to a single homogeneous phase occupying the entire macroscopic system. The initial appearance of broken chiral symmetry that occurs upon lowering the temperature below $T_\pm$ can be illustrated by setting

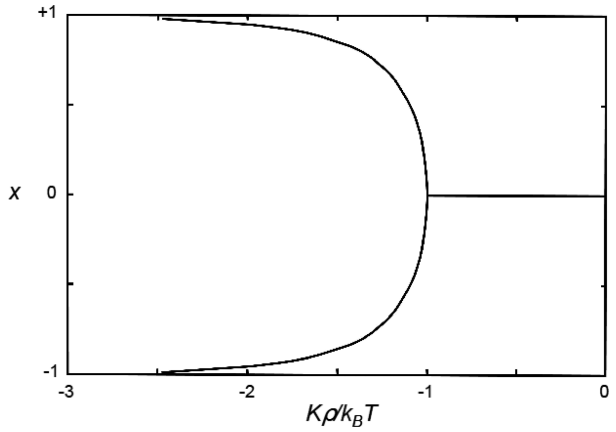

Figure 1. Numerical values of chirality intensity variable x *vs* the coupling parameter $K\rho/k_BT$, determined by eq 11.

$$K\rho/k_BT = -1 - \varepsilon \tag{13}$$

where $\varepsilon \geq 0$. Then by carrying out x expansions to fourth order for both the left and right members of eq 11, one finds that the leading-order extent of chiral symmetry breaking is described by

$$x = \pm(3\varepsilon)^{1/2} + O(\varepsilon^{3/2}) \tag{14}$$

a behavior graphically evident in Figure 1.

V. LIQUID–VAPOR TRANSITION

The next step involves assuming that coupling constant J is negative, while for the coverage fraction $\rho = N/M$ and temperature T ranges to be considered now, the other coupling constant K is sufficiently weak by comparison that spontaneous chiral symmetry breaking has not yet occurred. In other words, for this section the dominant term in the configurational partition function will remain at $x = 0$ ($N_+ = N_- = N/2$). Therefore, eq 10 simplifies to produce the following relevant expression:

$$\begin{aligned} -F/k_BT \approx N\ln\omega + M\ln M - (M - N)\ln(M - N) \\ - N\ln\left(\frac{N}{2}\right) - \left(\frac{JN^2}{2Mk_BT}\right) \end{aligned} \tag{15}$$

To locate any liquid–vapor critical point exhibited by cooling the racemic fluid, it is necessary to examine the equilibrium pressure equation of state as the lattice coverage fraction varies. The pressure p can be extracted from F by an isothermal volume derivative:

$$\begin{aligned} p &= -\left(\frac{\partial F}{\partial V}\right)_{N,T} \\ &\approx -\frac{1}{\omega}\left(\frac{\partial F}{\partial M}\right)_{N,T} \end{aligned} \tag{16}$$

where the lattice model volume measure ωM can be treated as a continuous variable for the macroscopic system size regime of interest. Consequently, eq 15 leads to the following simple expression:

$$p\omega = -k_BT\ln(1 - \rho) + J\rho^2/2 \tag{17}$$

where $\rho = N/M$ continues to represent the particle number density on a per-cell basis.

DOI: 10.1021/acs.jpcb.7b10498
J. Phys. Chem. B 2018, 122, 3441−3446

The existence of a liquid−vapor critical point and its associated phase separation rest upon the stated condition $J < 0$. Their locations within the mean field approximation can be obtained by plotting the family of pressure vs volume curves, or more specifically the $p\omega$ vs $1/\rho$ curves. The critical point is the location of the highest-temperature occurrence of a vanishing slope of these curves for $0 < \rho < 1$, to be determined by

$$0 = \left(\frac{\partial p\omega}{\partial(1/\rho)}\right)_T = -\rho^2\left(\frac{\partial p\omega}{\partial \rho}\right)_T = \left(\frac{\rho^2}{1-\rho}\right)[J\rho^2 - J\rho - k_B T] \quad (18)$$

From the zeroes of the second factor in the last expression, that condition implies

$$\rho = (1/2)\{1 \pm [1 + (4k_B T/J)]^{1/2}\} \quad (19)$$

so that locating the liquid−vapor critical point temperature T_{lv} requires the two solutions to coincide, i.e.

$$k_B T_{lv} = -J/4$$
$$\rho_{lv} \equiv (N/M)_{lv} = 1/2 \quad (20)$$

This single critical point location in the T, ρ plane for fixed J contrasts qualitatively with the continuous chiral-symmetry-breaking critical point set $T_{\pm}(\rho)$ for fixed $K < 0$ described earlier by eq 12.

If the temperature were to decline below T_{lv}, for which one can then write $(\eta > 0)$

$$4k_B T/J = -1 + \eta \quad (21)$$

then the split pair of densities, at which the vanishing derivatives via eq 18 formally occur, locate the spinodal curves generated by the mean field approximation:

$$\rho_{sp} = (1/2)[1 \pm \eta^{1/2}] \quad (22)$$

However, more direct relevance for the present investigation involves the prediction of the temperature dependence of the liquid−vapor equilibrium coexistence densities ρ_l and ρ_v. These can be extracted from the p_ω vs $1/\rho$ family of curves by using the Maxwell equal-areas construction,[7] which assures equality of chemical potential for the two coexisting racemic fluids. The leading-order results for small η only require locally approximating the curve shapes through cubic order in $1/\rho$, with the result

$$\rho_l, \rho_v = (1/2)[1 \pm (3\eta)^{1/2}] + O(\eta) \quad (23)$$

Figure 2 provides a schematic isochoric $(\rho = 1/2)$ scenario of the liquid−vapor critical region, showing as well a separate lower-temperature, higher-density critical point for the chiral symmetry breaking phenomenon. The curves appearing in the three-dimensional space of absolute temperature T, density ρ, and chiral asymmetry x, represent the properties of the individual homogeneous phases, portions of which can simultaneously be present. Under the isochoric constraint $\rho = 1/2$ for appearance of the liquid−vapor critical point, the thermodynamic equilibrium states that have been subject to the phase transitions would involve coexistence of macroscopic quantities of those homogeneous phases in relative amounts conforming to the overall isochoric constraint. In this connection it is worth noting that three distinct fluid−fluid

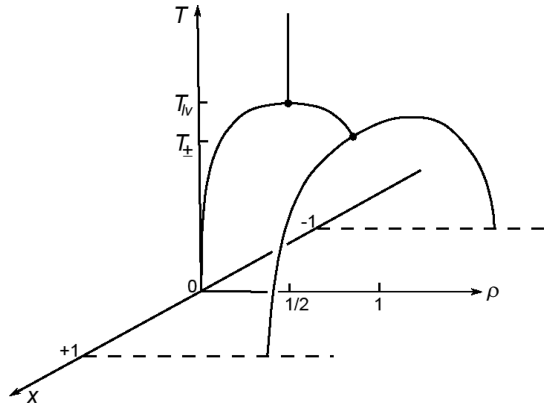

Figure 2. Isochoric scenario indicating both a high temperature liquid−vapor critical point at T_{lv}, and a lower temperature, higher density, chiral-symmetry- breaking critical point at $T_{\pm}$. The curves shown in this T, ρ, x space represent the intensive properties of the homogeneous phases that would appear simultaneously under the coexistence conditions enforced by the system's overall isochoric constraint, $\rho = 1/2$.

interfaces will appear, each with its own characteristic temperature-dependent surface tension. These are associated respectively with (a) the liquid−vapor coexistence for the racemic fluids just below their critical point at T_{lv}, (b) the contact interface between the coexisting opposite-chirality isotropic liquids for $T < T_{\pm}$ as determined by the applicable $\rho_l(T)$, and (c) the chiral-liquid, racemic-vapor interface at coexistence, also for $T < T_{\pm}$.

It should be mentioned that the existence of the chirality-emergence phase transition would be accompanied by a change in the temperature dependence of the vapor pressure, which in principal would influence the $T < T_{\pm}$ shape of the racemic vapor phase curve that is present in Figure 2. In the low temperature limit, that racemic vapor phase approaches $\rho = 0$, while the chiral liquids in that temperature limit approach $\rho = 1$, $x = \pm 1$.

VI. CRITICAL POINT CONFLUENCE

Increasing the magnitude of an initially small negative coupling constant K while holding $J < 0$ fixed obviously causes $T_{\pm}$ to drift upward toward T_{lv}. By comparing eqs 12 and 20, one sees that these critical temperatures become coincident at density $\rho = 1/2$ when those negative coupling constants J and K obey

$$K = J/2 \quad (24)$$

This of course constitutes confluence (cfl) of the two otherwise distinct critical points to produce a single qualitatively novel critical feature for J, $K < 0$ located at

$$k_B T_{cfl} = -J/4 = -K/2$$
$$\rho_{cfl} = 1/2 \quad (25)$$

Note that this critical point confluence situation would cause three distinct fluid phases to emerge continuously from the single critical point as the high-temperature $\rho = 1/2$ racemic fluid is cooled isochorically through that temperature point. Figure 3 schematically illustrates these coexisting phases (racemic vapor, and two opposite-chirality isotropic liquids) emanating from the common critical point. As a result of this critical point confluence, now only two distinct interfaces and their corresponding surface tensions are present: (a) the

DOI: 10.1021/acs.jpcb.7b10498
J. Phys. Chem. B 2018, 122, 3441−3446

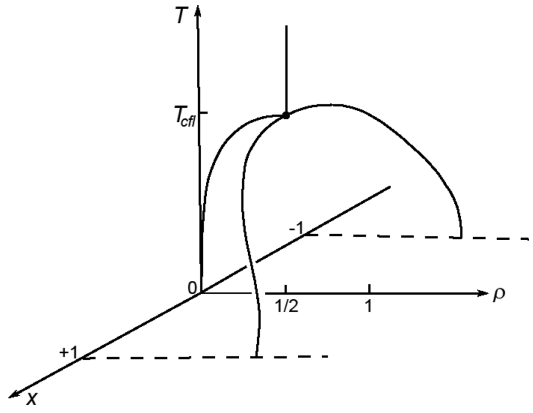

Figure 3. Isochoric ($\rho = 1/2$) emergence pattern of three coexisting homogeneous fluid phases, indicating their intensive properties in the T, ρ, x space when the negative coupling parameters J and K are chosen to cause confluence of the critical points, eqs 24 and 25.

racemic-vapor, chiral liquid coexistence contact and (b) coexistence contact of the two isotropic opposite-chirality liquids.

A basic issue is whether the critical point confluence qualitatively affects the shapes of the coexistence curves just below that critical point. Note that condition (24) leads to a simplified version of the free energy expression, eq 10:

$$\begin{aligned} -F(M,N,T)/Nk_BT &\approx \ln\omega + \left(\frac{M}{N}\right)\ln\left(\frac{M}{N}\right) - \left(\frac{M}{N}-1\right)\ln\left(\frac{M}{N}-1\right) \\ &\quad + \ln 2 - \left(\frac{JN}{2Mk_BT}\right) + \frac{1}{2}\underbrace{\max}_{x}\left\{-(1+x)\ln(1+x)\right. \\ &\quad \left. -(1-x)\ln(1-x) - \left(\frac{JN}{2Mk_BT}\right)x^2\right\} \end{aligned} \tag{26}$$

from which a trivially modified version of eq 11 arises:

$$\frac{1+x}{1-x} = \exp\left[-\left(\frac{J\rho}{k_BT}\right)x\right] \tag{27}$$

In eq 26 the maximum-producing chiral symmetry breaking parameter x will deviate from zero provided that $\varepsilon > 0$, where now

$$\begin{aligned} \varepsilon &= (-J\rho/2k_BT) - 1 \\ &= \left[\frac{1+2\Delta\rho}{1-(4k_B/J)\Delta T}\right] - 1 \end{aligned} \tag{28}$$

showing explicitly how the extended definition of this quantity from eq 13 depends on the density and temperature deviations from the location of the confluent critical point:

$$\begin{aligned} \rho &= \rho_{cfl} + \Delta\rho \\ T &= T_{cfl} + \Delta T \end{aligned} \tag{29}$$

The configurational free energy now takes the following form:

$$\begin{aligned} -F/k_BT \approx{}& N\ln\omega + M\ln M - (M-N)\ln(M-N) \\ & - N\ln(N/2) + N(1+\varepsilon) + (3N\varepsilon^2/4)\theta(\varepsilon) \end{aligned} \tag{30}$$

where the specific version shown for the last term is its leading-order contribution in ε, which is sufficient to establish the system's behavior just below the confluent critical point. The Heaviside unit step function θ has been incorporated to ensure that this last term contributes to F only when $\varepsilon > 0$.

The system pressure can again be obtained from F by a volume derivative, and the Maxwell equal-areas construction[7] can again be used to guarantee that the coexisting phases below the confluent critical point possess the same chemical potential. For states with $\varepsilon < 0$, the previous pressure eq 17 still applies. However, the additional contribution for $\varepsilon > 0$, the last term in eq 30, provides additional cohesive stabilization for the chiral liquid, thus reducing its pressure. This depression naturally influences the Maxwell construction, causing at a fixed $\Delta T < 0$ a wider separation between the densities of coexisting racemic vapor and chiral liquid. However, this effect arises just from a fractionally small increase in liquid binding, compared to that already present at the confluent critical point. Therefore, the same mean-field-predicted coexistence density exponent 1/2, as appeared in eq 23, still applies for the system's behavior just below the confluent critical point.

However, a qualitatively different outcome emerges from the critical behavior of the extent of chiral symmetry breaking. This arises in connection with the density variation of $T_{\pm}$ indicated earlier, eq 12. As a result of the confluence, the chiral symmetry breaking phenomenon is not subject to a fixed number density ρ, but to the liquid density rising by an amount proportional to $|\Delta T|^{1/2}$ as T declines. Consequently, the applicable parameter x exhibits the following leading-order temperature dependence:

$$\begin{aligned} x &\cong \pm(3\varepsilon)^{1/2} \\ &\propto \pm(\Delta\rho)^{1/2} \\ &\propto \pm(|\Delta T|^{1/2})^{1/2} \\ &= \pm|\Delta T|^{1/4} \end{aligned} \tag{31}$$

This reduction of the chiral symmetry breaking critical exponent by a factor of 2 constitutes a distinctive characteristic of critical point confluence for the two different types of particle segregations driven by the negative interaction parameters J and K.

VII. CONCLUDING REMARKS

Having discussed the effects at the half-filled density $\rho = 1/2$ of raising the chiral-symmetry-breaking critical point temperature $T_{\pm}$ from substantially below T_{lv} until these two coincide, it is natural to inquire whether continuation at the same overall system density 1/2 can yield a nontrivial situation where again two critical points appear with $T_{\pm} > T_{lv}$. A straightforward analysis indicates that upon isochoric cooling, an initially high-temperature chiral liquid at this density 1/2 would not exhibit a liquid–vapor critical point. Instead, cooling the chiral liquid phase would cause its pressure to decline until it equaled an equilibrium vapor pressure, at which point a first-order vaporization transition would occur. In other words, when $|2K| > |J|$, the high temperature chirality occurrence pre-empts appearance of a conventional liquid–vapor critical point.

Although the mean-field approximation for the present three-dimensional model should be expected to yield qualitatively

DOI: 10.1021/acs.jpcb.7b10498
J. Phys. Chem. B 2018, 122, 3441−3446

reasonable results, it obviously would be desirable to compare those results with the corresponding predictions of more sophisticated approaches. Specifically, it would be useful to apply Monte Carlo numerical simulations of the lattice model to test the accuracy of the various predictions offered in the previous sections IV–VI above. One important aspect of such a comparison would be to establish numerically the effects of varying the spatial ranges of the pair interaction functions φ_J and φ_K.

The extensive history of work devoted to critical exponents[8] has revealed the imprecision of the mean field predictions in three-dimensional cases involving finite range pair interactions. Specifically, the square-root results for coexistence curve shapes in eqs 14 and 23 above are expected to be reduced to approximately 5/16. The renormalization group formalism[9,10] certainly deserves to be applied here, and the unusual critical point confluence exponent estimated to be 1/4 in eq 31 would be a novel case for analysis by the renormalization group approach.

Although not directly the object of this study, it was pointed out above that several cases of interfacial tension arise in the present model for contact between coexisting fluid phases. Determining the temperature dependence ($\propto|\Delta T|^{\mu}$) of those fluid pairs emerging directly from a single or a confluent critical point would be a sensible objective for future research. In particular, it would certainly be informative to compare exponent μ results for the present model to the critical exponent extracted from experimental measurements on conventional fluids in the neighborhood of their conventional liquid–vapor critical points:[11]

$$\mu \cong 1.26 \cong 5/4 \tag{32}$$

An inevitable final comment is that sustained experimental effort might well be expended to broaden the range of known flexible molecular substances that exhibit coexisting isotropic chiral liquids. This would enhance the likelihood of encountering experimentally the kind of critical point confluence that the present simple spin-1 Ising model has been constructed to illuminate.

AUTHOR INFORMATION

Corresponding Author

*E-mail: fhs@princeton.edu.

ORCID

Frank H. Stillinger: 0000-0002-1225-8186

Notes

The author declares no competing financial interest.

ACKNOWLEDGMENTS

The author is indebted to Prof. P.G. Debenedetti, Princeton University, for many insightful discussions concerning molecular chirality and its symmetry-breaking phenomena.

REFERENCES

(1) Ellis, C. M. The 2-Butoxyethanol-Water System. Critical Solution Temperatures and Salting-Out Effects. *J. Chem. Educ.* **1967**, *44*, 405–407.

(2) Andersen, G. R.; Wheeler, J. C. Directionality Dependence of Lattice Models for Solutions with Closed Loop Coexistence Curves. *J. Chem. Phys.* **1978**, *69*, 2082–2088.

(3) Dressel, C.; Reppe, T.; Prehm, M.; Brautzsch, M.; Tschierske, C. Chiral Self-Sorting and Amplification in Isotropic Liquids of Achiral Molecules. *Nat. Chem.* **2014**, *6*, 971–977.

(4) Dressel, C.; Weissflog, W.; Tschierske, C. Spontaneous Mirror Symmetry Breaking in a Re-Entrant Isotropic Liquid. *Chem. Commun.* **2015**, *51*, 15850–15853.

(5) Latinwo, F.; Stillinger, F. H.; Debenedetti, P. G. Molecular Model for Chirality Phenomena. *J. Chem. Phys.* **2016**, *145*, 154503.

(6) Blume, M.; Emery, V. J.; Griffiths, R. B. Ising Model for the λ Transition and Phase Separation in $He^3 - He^4$ Mixtures. *Phys. Rev. A: At., Mol., Opt. Phys.* **1971**, *4*, 1071–1077.

(7) Huang, K. *Statistical Mechanics*; John Wiley & Sons: New York, 1963; p 44.

(8) Fisher, M. E. The Theory of Equilibrium Critical Phenomena. *Rep. Prog. Phys.* **1967**, *30*, 615–730.

(9) Maris, H. J.; Kadanoff, L. P. Teaching the Renormalization Group. *Am. J. Phys.* **1978**, *46*, 652–657.

(10) Fisher, M. E. Renormalization Group Theory: Its Basis and Formulation in Statistical Physics. *Rev. Mod. Phys.* **1998**, *70*, 653–681.

(11) Rowlinson, J. S.; Widom, B. *Molecular Theory of Capillarity*; Clarendon Press: Oxford, 1982; pp 264–265.

DOI: 10.1021/acs.jpcb.7b10498
J. Phys. Chem. B 2018, 122, 3441–3446